Dynamics of Chemoimmunotherapy Models

Lakshmi N Sridhar

Chemical Engineering Department, University of Puerto Rico, Mayaguez, PR 00681, USA

Abstract

Chemoimmunotherapy is chemotherapy combined with immunotherapy. Chemotherapy uses different drugs to kill or slow the growth of cancer cells; immunotherapy uses treatments to stimulate or restore the ability of the immune system to fight cancer. Both chemotherapy and immunotherapy are highly nonlinear processes that several factors affect. The two treatments together would be very highly nonlinear. It is necessary to understand and control this combined treatment. Bifurcation analysis is a powerful mathematical tool used to deal with the nonlinear dynamics of any process. Several factors must be considered, and multiple objectives must be met simultaneously. Bifurcation analysis and multiobjective nonlinear model predictive control (MNLMPC) calculations are performed on two chemoimmunotherapy models. The MATLAB program MATCONT was used to perform the bifurcation analysis. The MNLMPC calculations were performed using the optimization language PYOMO in conjunction with the state-of-the-art global optimization solvers IPOPT and BARON.. The bifurcation analysis revealed branch and limit points in the two models. The branch and limit points were beneficial because they enabled the multiobjective nonlinear model predictive control calculations to converge to the Utopia point in both the problems, which is the best solution.

*Corresponding author: Lakshmi N Sridhar, Chemical Engineering Department, University of Puerto Rico, Mayaguez, PR 00681, USA.

Background

Buzaid developed strategies for combining chemotherapy and biotherapy in melanoma [1]. De Pillis and Radunskaya developed a mathematical tumor model with immune resistance and drug therapy [2]. Jackson discussed vascular tumor growth and treatment and the consequences of polyclonality, competition and dynamic vascular support [3]. Liu et al. investigated cell-mediated immunotherapy which is a new approach to the treatment of malignant glioma [4].

Chaplain discussed several mathematical models in cancer research [5].

De Pillis and Radunskaya, investigated the Immune response to tumor invasion [6]. Schirrmacher et al. discussed several models for immunotherapy and Cancer Vaccines [7]. Arciero et al. developed a mathematical model of tumor-immune evasion and siRNA treatment [8]. Burden et al. applied optimal control techniques to immunotherapy, Chao et al. developed a stochastic model of cytotoxic T cell responses [9,10]. Matzavinos Chaplain performed a travelling-wave analysis of a model of the immune response to cancer [11].

Matzavinos et al. developed mathematical models of the spatiotemporal response of cytotoxic T-lymphocytes to a solid tumor [12]. Garbelli et al. discussed the Melanocyte-specific, cytotoxic T cell responses in vitiligo studying the effective variant of melanoma immunity [13]. Wheeler et al. investigated the Clinical responsiveness of glioblastoma multiforme to chemotherapy after vaccination [14]. Li et al. researched the generation of PRL-3- and PRL-1-specific monoclonal antibodies as potential diagnostic markers for cancer metastases [15].

Qu et al. investigated the Development of humanized antibodies as cancer therapeutics [16]. De Pillis et al. theoretically investigated the mixed immunotherapy and chemotherapy of tumors [17]. Malleta and De Pillis developed a cellular automata model of tumor–immune system interactions [18]. De Pillis et al. performed a theoretical investigation of chemotherapy for tumors, and Isaeva et al. discussed the different strategies for cancer treatment [19,20]. Ledzewicz et al. developed optimal controls for a mathematical model of tumor-immune interactions under targeted chemotherapy with immune boost [21].

Eladdadi et al. developed mathematical models of tumor-immune system dynamics [22]. Wang et al. performed optimal control for a mathematical model for cancer chemotherapy under tumor heterogeneity [23]. Abdel-Wahab et al. discussed the adverse events in cancer immunotherapy [24]. Lai, and Friedman discussed the combination therapy of cancer with cancer vaccine and immune checkpoint inhibitors [25]. Ratajczyk et al. performed optimal control for a mathematical model of glioma treatment with oncolytic therapy and TNF-α inhibitors [26]. Guti´errez-Diez and Russo disussed the design of personalized cancer treatments by use of optimal control for he case of chronic myeloid leukemia [27]. Khajanchi investigated the impact of immunotherapy on a glioma immune interaction model [28]. Takacs et al. demonstrated that the modulation of the chemokine/chemokine receptor axis was a novel approach for glioma therapy [29].

Liu et al. performed a dynamics analysis of a tumor-immune system with chemotherapy [30]. Anderson et al. showed that global stability and parameter analysis reinforce therapeutic targets of PD-L1-PD-1 and MDSCs for glioblastoma [31]. Cherraf et al. mathematically modelled the tumor–immune system with time delay and diffusion [32]. Luo et al. discussed the optimal treatment strategy for cancer based on mathematical modeling and impulse control theory [33]. Anderson et al. performed optimal control of combination immunotherapy for a virtual murine cohort in a glioblastoma-immune dynamics model [34].

All optimal control work involving chemoimmunotherapy models involve single-objective optimal control. The main objective of this paper is to perform multiobjective nonlinear model predictive control(MNLMPC) in conjunction with bifurcation analysis for two chemoimmunotherapy models. The two models that will be used are those described in Anderson et al. and the scaled model in Isaeva et al. This paper is organized as follows [34,20]. First the model equations are presented. The numerical procedures (bifurcation analysis and multiobjective nonlinear model predictive control (MNLMPC) are then described. This is followed by the results and discussion and conclusions.

Chemoimmunotherapy Models
The two models that are presented in Anderson et. al.. (2024) [34] and the scaled model in Isaeva et al (2009)[20] will be used for the calculations. These models will be briefly described in this section.

Model 1 (Anderson et al. [34])
The model equations are

$$\frac{dc_{val}}{dt} = \lambda_c c_{val}(1 - \frac{c_{val}}{c_{max}}) - \eta t_{val} c_{val}$$

$$\frac{dt_{val}}{dt} = -r t_{val} m_{val} - d_t t_{val} + \frac{(\alpha_T + s_T t_{val} c_{val})}{1 + \rho(t_{val} + \varepsilon_C c_{val})(1 - u_1(t) t_{val})}$$

$$\frac{dm_{val}}{dt} = s_m c_{val}(1 - u_2(t) t_{val}) - d_m m_{val}$$

(1)

$c_{val}, t_{val}, m_{val}$ represent the tumor cells, activated T cells, and myeloid-derived suppressor cells (MDSCs).

The base parameters are

$\lambda_c = 0.25; \ c_{max} = 1.45e+07; \eta = 1.27e-07; \alpha_t = 2.45e+06;$
$s_t = 5.91e+06; \rho = 0.207; \varepsilon_c = 31.1; r = 1.83e-05; d_t = 0.415;$
$s_m = 0.0476; d_m = 0.263; \ u_1 = 0; u_2 = 0;$

For the bifurcation calculations λ_c was the

bifurcation parameter while $u_1 = 0; u_2 = 0$. For the MNLMPC calculations, $\lambda_c = 0.25$ while $u_1; u_2$ are the control variables.

Model 2 (Scaled model of Isaeva et al. [20])
The model equations are

$$\frac{dt_{val}}{dt} = -h_1 t_{val} \ln\left(\frac{h_2 t_{val}}{h_1}\right) - h_3 t_{val} l_{val}(2 - e^{-l_{val}}) - m_1 t_{val}(2 - e^{-l2_{val}})(1 - e^{-c_{val}})$$

$$\frac{dl_{val}}{dt} = h_4 + h_5 l_{val} I2_{val} - l_{val} - m_2 l_{val}(2 - e^{-l2_{val}})(1 - e^{-c_{val}})$$

$$\frac{dI2_{val}}{dt} = m_3(t) + \left(\frac{h_6 t_{val}}{t_{val} + h_9}\right) - h_7 l_{val} I2_{val} - h_8 t_{val} I2_{val}$$

$$\frac{dC_{val}}{dt} = m_4(t) - m_5 c_{val}$$

$$\frac{dI_{val}}{dt} = m_6(t) - m_7 I_{val}$$

(2)

$t_{val}, l_{val}, I2_{val}, C_{val}, I_{val}$ represent the dimensionless tumor cells, Cytotoxic T Lymphocytes, Interleukin-2, chemotherapeutic drug (C), and Interferon-alpha.

The scaled model parameters are

$h_1 = 0.3939, h_2 = 0.0909, h_3 = 1.5000, h_4 = 0.2458,$

$h_5 = 0.6061, h_6 = 3.6364, h_7 = 1.0091,$

$h_8 = 6.3636, h_9 = 0.0300, m_1 = 2.7273,$

$m_2 = 1.8182, m_5 = 19.3939, m_7 = 5.1515.$

m_3, m_4, m_6 were taken as individual bifurcation parameters (one at a time, with the other two being 0) and collectively as control parameters for the MNLMPC calculations.

Numerical Procedures
Bifurcation Analysis
The MATLAB software MATCONT is used to perform the bifurcation calculations. Bifurcation analysis deals with multiple steady-states and limit cycles. Multiple steady states occur because of the existence of branch and limit points. Hopf bifurcation points cause limit cycles. A commonly used MATLAB program that locates limit points, branch points, and Hopf bifurcation points is MATCONT [35,36]. This program detects Limit points(LP), branch points(BP), and Hopf bifurcation points(H) for an ODE system

$$\frac{dx}{dt} = f(x, \alpha)$$

(3)

$x \in R^n$ Let the bifurcation parameter be a Since the gradient is orthogonal to the tangent vector, The tangent plane at any point $w = [w_1, w_2, w_3, w_4, ... w_{n+1}]$ must satisfy

$$Aw = 0$$

(4)

Where A is $A = [\partial f / \partial x \ \ | \partial f / \partial \alpha]$ (5)

where $\partial f / \partial x$ is the Jacobian matrix. For both limit and branch points, the matrix $[\partial f / \partial x]$ must be singular. The n+1 th component of the tangent vector $w_{n+1} = 0$ for a limit point (LP)and for a branch point (BP) the matrix must be singular. At a Hopf bifurcation point,

$$\det(2 f_x(x, \alpha) @ I_n) = 0$$

(6)

@ indicates the bialternate product while I_n is the n-square identity matrix. Hopf bifurcations cause limit cycles and should be eliminated because limit cycles make optimization and control tasks very difficult. More details can be found in Kuznetsov and Govaerts [37-39].

Multiobjective Nonlinear Model Predictive Control (MNLMPC)

Flores Tlacuahuaz et al. developed a multiobjective nonlinear model predictive control (MNLMPC) method that is rigorous and does not involve weighting functions or additional constraints [40]. This procedure is used for performing the MNLMPC calculations Here $\sum_{t_i=0}^{t_i=t_f} q_j(t_i)$ (j=12..n) represents the variables that need to be minimized/maximized simultaneously for a problem involving a set of ODE

$$\frac{dx}{dt} = F(x,u) \tag{7}$$

t_f being the final time value, and n the total number of objective variables and u the control parameter. This MNLMPC procedure first solves the single objective optimal control problem independently optimizing each of the variables $\sum_{t_i=0}^{t_i=t_f} q_j(t_i)$ individually. The minimization/maximization of $\sum_{t_i=0}^{t_i=t_f} q_j(t_i)$ will lead to the values q_j^*. Then the optimization problem that will be solved is

$$\min(\sum_{j=1}^{n} (\sum_{t_i=0}^{t_i=t_f} q_j(t_i) - q_j^*))^2$$
$$subject\ to\ \frac{dx}{dt} = F(x,u); \tag{8}$$

This will provide the values of u at various times. The first obtained control value of u is implemented and the rest are discarded. This procedure is repeated until the implemented and the first obtained control values are the same or if the Utopia point where

$$(\sum_{t_i=0}^{t_i=t_f} q_j(t_i) = q_j^* \text{ for all j)} \text{ is Obtained}$$

Pyomo is used for these calculations [41]. Here, the differential equations are converted to a Nonlinear Program (NLP) using the orthogonal collocation method The NLP is solved using IPOPT and confirmed as a global solution with BARON [42,43].

The steps of the algorithm are as follows

1. Optimize $\sum_{t_i=0}^{t_i=t_f} q_j(t_i)$ and obtain q_j^* at various time intervals ti. The subscript i is the index for each time step.

2. Minimize $(\sum_{j=1}^{n}(\sum_{t_i=0}^{t_i=t_f} q_j(t_i) - q_j^*))^2$ and get the control values for various times.

3. Implement the first obtained control values

4. Repeat steps 1 to 3 until there is an insignificant difference between the implemented and the first obtained value of the control variables or if the Utopia point is achieved. The Utopia point is when

Sridhar proved that the MNLMPC calculations to converge to the Utopia solution when the bifurcation analysis revealed the presence of limit and branch points [44]. This was done by imposing the singularity condition on the co-state equation [45].

If the minimization of q_1 lead to the value q_1^* and the minimization of q_2 lead to the value q_2^* The MNLPMC calculations will minimize the function $(q_1-q_1^*)^2 + (q_2-q_2^*)^2$. The multiobjective optimal control problem is

$$\min \quad (q_1-q_1^*)^2 + (q_2-q_2^*)^2 \quad subject\ to\ \frac{dx}{dt} = F(x,u) \tag{9}$$

Differentiating the objective function results in

$$\frac{d}{dx_i}((q_1-q_1^*)^2 + (q_2-q_2^*)^2) = 2(q_1-q_1^*)\frac{d}{dx_i}(q_1-q_1^*) + 2(q_2-q_2^*)\frac{d}{dx_i}(q_2-q_2^*) \tag{10}$$

The Utopia point requires that both $(q_1-q_1^*)$ and $(q_2-q_2^*)$ are zero. Hence

$$\frac{d}{dx_i}((q_1-q_1^*)^2 + (q_2-q_2^*)^2) = 0 \tag{11}$$

the optimal control co-state equation (Upreti; 2013) is

$$\frac{d}{dt}(\lambda_i) = -\frac{d}{dx_i}((q_1 - q_1^*)^2 + (q_2 - q_2^*)^2) - f_x\lambda_i; \quad \lambda_i(t_f) = 0 \quad (12)$$

λ_i is the Lagrangian multiplier. t_f is the final time. The first term in this equation is 0 and hence

$$\frac{d}{dt}(\lambda_i) = -f_x\lambda_i; \lambda_i(t_f) = 0 \qquad (13)$$

At a limit or a branch point, for the set of ODE

$\frac{dx}{dt} = f(x,u)$ f_x is singular. Hence there are two different vectors-values for

$[\lambda_i]$ where $\frac{d}{dt}(\lambda_i) > 0$ and $\frac{d}{dt}(\lambda_i) < 0$ .In between there is a vector

$[\lambda_i]$ where $\frac{d}{dt}(\lambda_i) = 0$. This coupled with the boundary condition $\lambda_i(t_f) = 0$ will lead to $[\lambda] = 0$ This makes the problem an unconstrained optimization problem, and the only solution is the Utopia solution.

Hopf bifurcations cause unwanted oscillatory behavior and limit cycles. The tanh activation function (where a control value u is replaced by) $(u \tanh u / \varepsilon)$ is commonly used in neural nets Dubey et al. and Kamalov et al. and Szandała and optimal control problems to eliminate spikes in the optimal control profile [46-49]. Hopf bifurcation points cause oscillatory behavior. Oscillations are similar to spikes, and the results in Sridhar demonstrate that the tanh factor also eliminates the Hopf bifurcation by preventing the occurrence of oscillations. Sridhar explained with several examples how the activation factor involving the tanh function successfully eliminates the limit cycle causing Hopf bifurcation points [50]. This was because the tanh function increases the time period of the oscillatory behavior, which occurs in the form of a limit cycle caused by Hopf bifurcations.

Results and Discussion

In model 1, for the bifurcation calculations λ_c was the bifurcation parameter, and a branch point BP was found at $[c_{val}, t_{val}, m_{val}, \lambda_c] == (14500000, 0, 2624334.6, 0)$. Figure 1a shows the bifurcation diagram with this branch point.
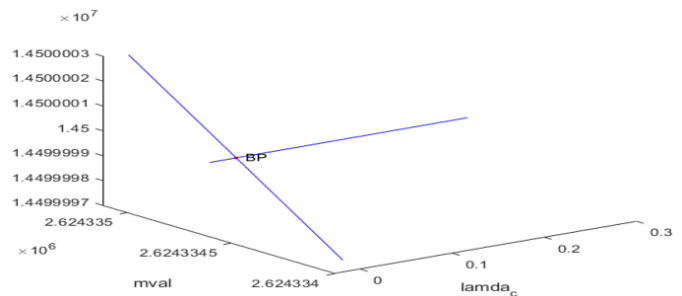

Figure 1a: Bifurcation Diagram for model 1

For the MNLMPC calculation, with u1 and u2 as the control variables. $\sum_{t_i=0}^{t_i=t_f} mval_j(t_i)$ was minimized, leading to a value of 0 and $\sum_{t_i=0}^{t_i=t_f} cval_j(t_i)$ was minimized also resulting in a value of 0. The overall optimal control problem will involve the minimization of

$$(\sum_{t_i=0}^{t_i=t_f} mval_j(t_i) - 0)^2 + (\sum_{t_i=0}^{t_i=t_f} cval_j(t_i) - 0)^2$$ subject to

the ODE describing Model 1

This minimization resulted in the Utopia point (0) confirming the analysis of Sridhar, which showed that the presence of a branch point enables the MNLMPC calculations to reach the best possible (Utopia) solution [34]. The first of the control variables is implemented and the rest are discarded. The process is repeated until the difference between the first and second values of the control variables are the same. This MNLMPC control values of u1 and u2 were 4.824e-07 and 0.4878. . The various MNLMPC profiles are shown in figure 1a and 1c.
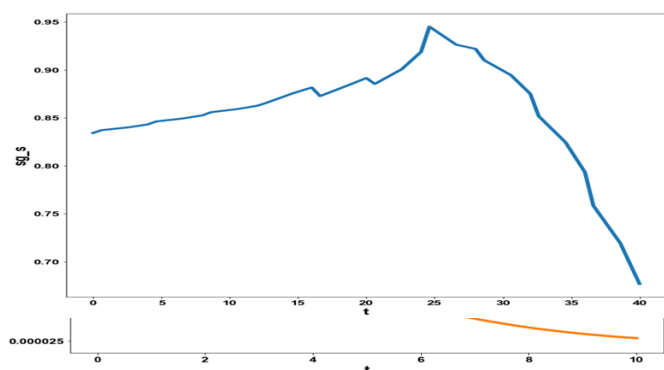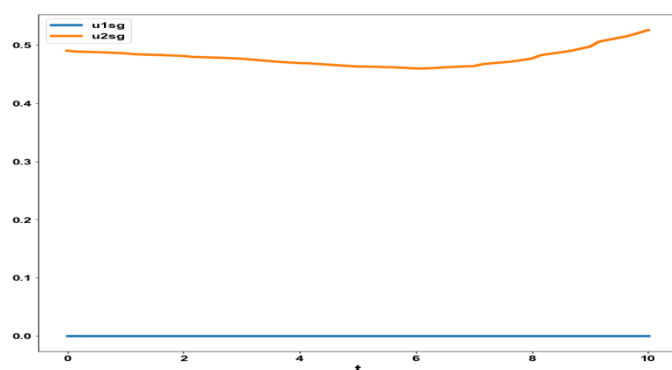
Figure 1c: cval , mval vs t (MNLMPC model 1)

The obtained control profile of s exhibited noise (figure 1d).
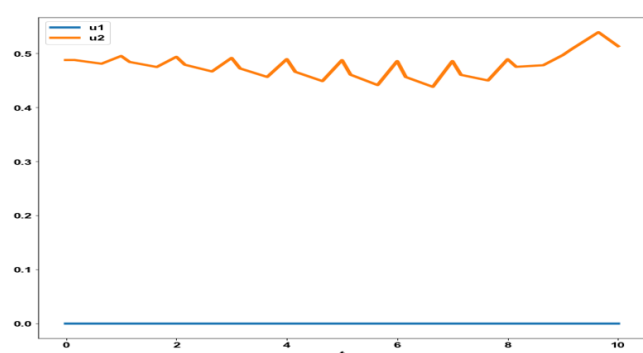
**Figure 1d: u1, u2 vs t (MNLMPC Model 1) some Noise is Observed**

This was remedied using the Savitzky-Golay Filter. The smoothed-out version of this profile is shown in Figure1e.


Figure 1e: u1, u2 vs t (MNLMPC Model 1) with Savitsky Golay filter

In model 2, m_3, m_4, m_6 each, when used as a bifurcation parameter, revealed the existence of a limit point. The coordinates for these $(t_{val}, l_{val}, I2_{val}, c_{val}, I_{val}, m_j)$ limit points j = 3,4,6 are
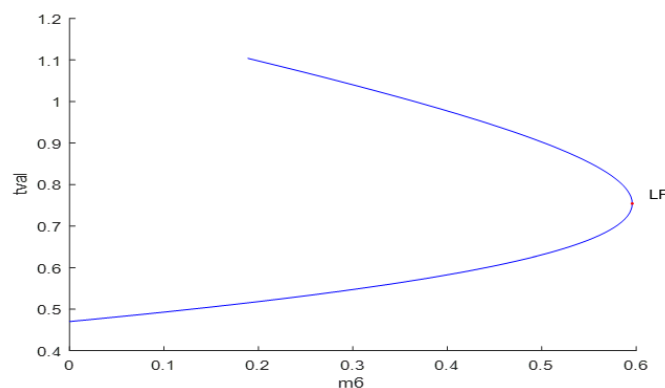(0.8622, 0.4240, 0.6935, 0.0, 0.0, 0.588); (0.5895, 0.3931, 0.8341, 0.047, 0.0, 0.9116) and

(0.7542, 0.4139, 0.6703, 0.0, 0.1156, 0.5957). Figures. 2a, 2b and 2c show the bifurcation diagrams for model 2.
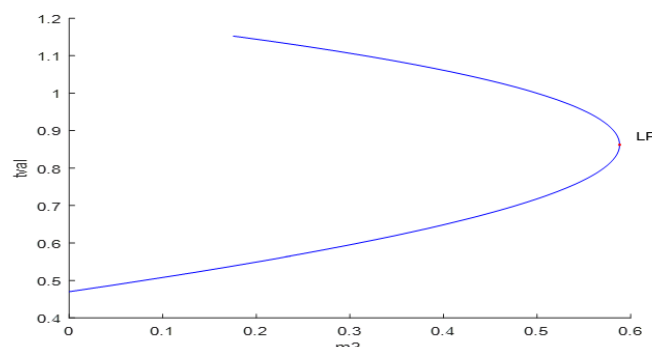
Figure 2a: Bifurcation Diagram for Model 2 (m3 as Bifurcation Parameter)
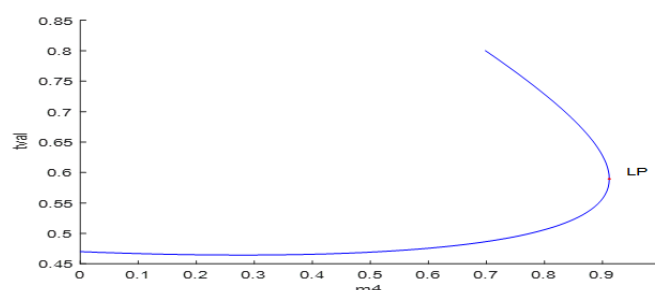
Figure 2b: Bifurcation Diagram for Model 2 (m4 as Bifurcation Parameter)

Figure 2c: Bifurcation Diagram for Model 2 (m6 as Bifurcation Parameter)

For the MNLMPC calculation, with m3 m4 and m6 s the control variables $\sum_{t_i=0}^{t_i=t_f} tval_j(t_i)$ was minimized, leading to a value of 3.45e-05 and $\sum_{t_i=0}^{t_i=t_f} lval_j(t_i)$ was maximized resulting in a value of 10.951. The overall optimal control problem will involve the minimization of

$$\left(\sum_{t_i=0}^{t_i=t_f} tval_j(t_i) - 3.45e-05\right)^2 + \left(\sum_{t_i=0}^{t_i=t_f} lval_j(t_i) - 10.951\right)^2$$

subject to the ODE describing Model 2. This minimization resulted in the Utopia point (0), confirming the analysis of Sridhar (2024a)[34], which showed that the presence of a branch point enables the MNLMPC calculations to reach the best possible (Utopia) solution. The first of the control variables is implemented, and the rest are discarded. The process is repeated until the difference between the first and second values of the control variables are the same. This MNLMPC control values of m3 m4 and m6 were 0.3491, 2.99977, 7.27841e-06. The various MNLMPC profiles are shown in figure 2d and 2e. The obtained control profile of s exhibited noise (figure 2f). This was remedied using the Savitzky-Golay Filter. The smoothed-out version of this profile is shown in Figure 2g.
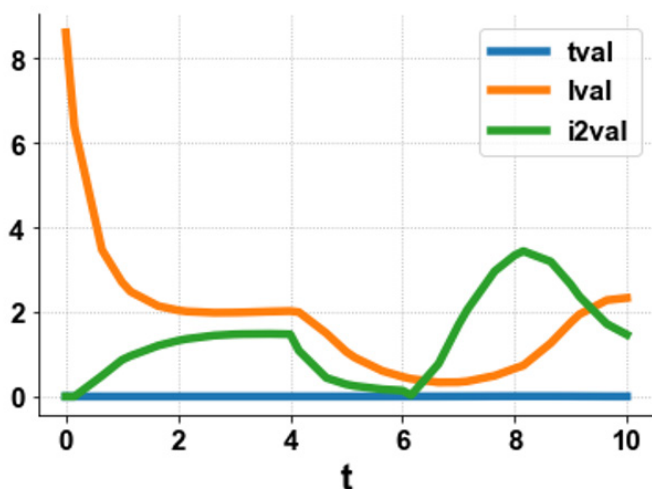

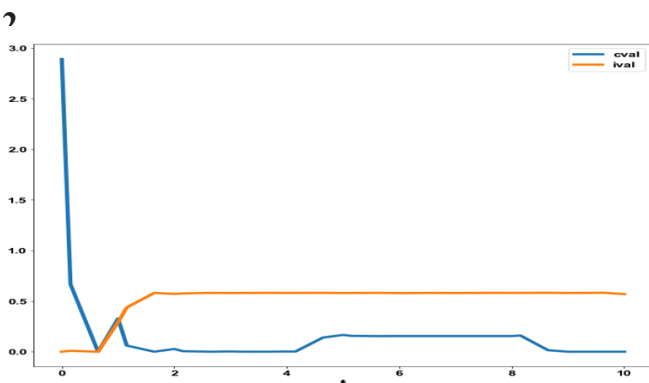**Figure 2d: tval, lval, i2val vs t (MNLMPC model 2**

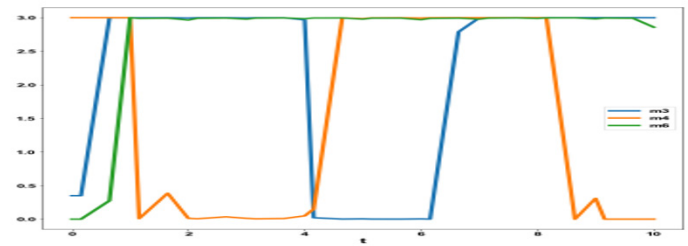**Figure 2e: cval, ival vs t (MNLMPC Model 2)**

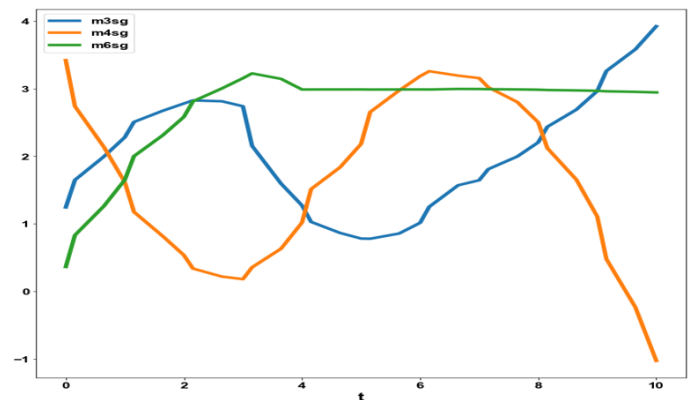**Figure 2f: m3 m4 m6 vs t (MNLMPC Model 1) some Noise is Observed.**

Figure 2g: m3, m4, m6 vs t (MNLMPC Model 2) with Savitsky-Golay Filter

Conclusions

Multiobjective nonlinear model predictive control calculations were performed along with bifurcation analysis on two chemoimmunotherapy models. The bifurcation analysis revealed the existence of limit and branch points that produced multiple steady-state solutions originating from a singular point. The limit and branch points are very beneficial as they caused the multiojective nonlinear model predictive calculations to converge to the Utopia point(the best possible solution) .in both models.

Data Availability Statement

All data used is presented in the paper

Conflict of Interest

The author, Dr. Lakshmi N Sridhar has no conflict of interest.

Acknowledgement

References

1. Buzaid AC (2000) Strategies for combining chemotherapy and biotherapy in melanoma, Cancer Control 7: 185-197.

2. De Pillis LG, A Radunskaya (2001) A mathematical tumor model with immune resistance and drug therapy: an optimal control approach, Journal of Theoretical Medicine 3: 79-100.

3. Jackson TL (2002) Vascular tumor growth and treatment: consequences of polyclonality, competition and dynamic vascular support, J. Math. Biol 44: 201-226.

4. Liu Y, Y Ng, KO Lillehei, Cell mediated immunotherapy: a new approach to the treatment of malignant glioma, Cancer Control 10: 138-147.

5. Chaplain MAJ (2003) Mathematical models in cancer research, in: The Cancer Handbook, Nature publishing group 60: 937-951.

6. De Pillis L G, AE Radunskaya (2003) Immune response to tumor invasion, in: Computational Fluid and Solid Mechanics, K. Bathe, eds, Cambridge: MIT Press 2: 1661-1668.

7. Schirrmacher V, V Umansky, M Linder, S Müerköster, M Rocha (2003) Models for immunotherapy and Cancer Vaccines, in: The Cancer Handbook, Nature publishing group 68: 1055-1068.

8. Arciero JC, DE Kirschner, TL Jackson (2004) A mathematical model of tumor-immune evasion and siRNA treatment, Disc. Cont. Dyn. Syst-B 4: 39-58.

9. Burden T, J Ernstberger, K Renee Fister (2004) Optimal control applied to immunotherapy, Discrete and Continuous dynamical systems-series B 4: 135-146.

10. Chao DL, MP Davenport, S Forrest, AS Perelson (2004) A stochastic model of cytotoxic T cell responses, Journal of Theoretical Biology 228: 227-240.

11. Matzavinos A, MAJ Chaplain (2004) Travelling-wave analysis of a model of the immune response to cancer, C R Biol 327: 995-1008.

12. Matzavinos A, MAJ Chaplain, VA Kuznetsov (2004) Mathematical modelling of the spatiotemporal response of cytotoxic T-lymphocytes to a solid tumour, Mathematical Medicine and Biology 21: 1-34.

13. Garbelli S, Mantovani B, Palermo, C Giachino (2005) Melanocyte-specific, cytotoxic T cell responses in vitiligo: the effective variant of melanoma immunity, Pigment Cell Res 18: 234-242.

14. Wheeler CJ, D Asha, L Genatao, JS Yu, KL (2005) Black, Clinical responsiveness of glioblastoma multiforme to chemotherapy after vaccination, Clin. Cancer Res 10: 5316-5326.

15. Li J, K Guo, VW Koh, JP Tang, BQ Gan, et al. (2005) Generation of PRL-3- and PRL-1-specific monoclonal antibodies as potential diagnostic markers for cancer metastases, Clin. Cancer Res 11: 2195-2204.

16. Qu Z, GL Griffiths, WA Wegener, CH Chang, SV Govindan, et al. (2005) Development of humanized antibodies as cancer therapeutics, Methods 36: 84-95.

17. De Pillis LG, W Gu, AE Radunskaya (2006) Mixed immunotherapy and chemotherapy of tumors: modeling, applications and biological interpretations, J. of Theoretical Biology 238: 841-862.

18. Malleta DG, LG de Pillis (2006) A cellular automata model of tumor–immune system interactions, J. of Theor. Biol 239: 334-350.

19. De Pillis LG, W Gu, KR Fister, T Head, K Maples (2007) Chemotherapy for tumors: an analysis of the dynamics and a study of quadratic and linear optimal controls, Mathematical Biosciences, 209: 292-315.

20. Isaeva OG, Osipov VA (2009) Different Strategies for Cancer Treatment: Mathematical Modelling. Computational and Mathematical Methods in Medicine 10: 253-272.

21. Ledzewicz U, Mosalman MSF, Sch¨attler H (2013) Optimal controls for a mathematical model of tumor-immune interactions under targeted chemotherapy with immune boost. Discrete Cont. Dyn. B 18: 1031-1051.

22. Eladdadi A, Kim P, Mallet D (2014) Mathematical models of tumor-immune system dynamics.. Springer, New York, NY 107.

23. Wang S, Schattler H (2016) Optimal control of a mathematical model forcancer chemotherapy under tumor heterogeneity. Math. Biosci. Eng 13: 1223-1240.

wW595: 111951.

24. Abdel-Wahab N, Alshawa A, Suarez-Almazor ME (2017) Adverse events in cancer immunotherapy. Adv. Exp. Med. Biol 155-174.

25. Lai X, Friedman A (2017) Combination therapy of cancer with cancer vaccine and immune checkpoint inhibitors: A mathematical model. PLoS One 12: e0178479.

26. Ratajczyk E, Ledzewicz U, Schattler H (2018) Optimal control for a mathematical model of glioma treatment with oncolytic therapy and TNF-α inhibitors. J. Optim. Theory Appl 176: 456-477.

27. Gutierrez-Diez PJ, Russo J (2020) Design of personalized cancer treatments by use of optimal control problems: The case of chronic myeloid leukemia. Math. Biosci. Eng 17: 4773-4800.

28. Khajanchi S (2021) The impact of immunotherapy on a glioma immune interaction model. Chaos Soliton Fract 152: 111346.

29. Takacs GP, Flores-Toro JA, Harrison JK (2021) Modulation of the chemokine/chemokine receptor axis as a novel approach for glioma therapy. Pharmacol. Ther 222: 107790.

30. Liu H, Yang H, Yang L (2021) Dynamics analysis in a tumor-immune system with chemotherapy. Chin. Phys. B 30: 058201.

31. Anderson HG, Takacs GP, Harris DC, Kuang Y, Harrison JK, et al. (2023) Global stability and parameter analysis reinforce therapeutic targets of PD-L1-PD-1 and MDSCs for glioblastoma. J. Math.Biol 88: 10.

32. Cherraf A, Li M, Moulai-Khatir A, Hamidaoui M (2023) Mathematical modeling of the tumor–immune system with time delay and diffusion. Axioms 12: 184.

33. Luo W, Tan X, Shen J (2023) Optimal treatment strategy for cancer based on mathematical modeling and impulse control theory. Axioms 12: 916.

34. Anderson HG, Gregory P, Takacs Jeffrey, K Harrison, Libin Rong, et al. (20204) Optimal control of combination immunotherapy for a virtual murine cohort in a glioblastoma-immune dynamics model,Journal of Theoretical Biology

35. Dhooge A, Govearts W, Kuznetsov AY (2003) MATCONT: "A Matlab package for numerical bifurcation analysis of ODEs", ACM transactions on Mathematical software 29: 141-164.

36. Dhooge AW, Govaerts YA, Kuznetsov W, Mestrom, AM Riet (2004) "CL_MATCONT"; A continuation toolbox in Matlab.

37. Kuznetsov YA (1998) Elements of applied bifurcation theory. Springer, NY.

38. Kuznetsov YA (2009) Five lectures on numerical bifurcation analysis, Utrecht University NL.

39. Govaerts JF (2000) Numerical Methods for Bifurcations of Dynamical Equilibria. SIAM.

40. Flores-Tlacuahuac A (2012) Pilar Morales and Martin Riveral Toledo; "Multiobjective Nonlinear model predictive control of a class of chemical reactors" . I & EC research 5891-5899.

41. Hart William E, Carl D, Laird, Jean-Paul Watson, David L (2021) Woodruff, Gabriel A. Hackebeil, Bethany L. Nicholson, and John D. Siirola. "Pyomo – Optimization Modeling in Python" Second Edition 67.

42. Wächter A, Biegler L (2006) On the implementation of an interior-point filter line-search algorithm for large-scale nonlinear programming. Math. Program 106: 25-57.

43. Tawarmalani M, NV Sahinidis (2005) A polyhedral branch-and-cut approach to global optimization", Mathematical Programming 103: 225-249.

44. Sridhar LN (2024) Coupling Bifurcation Analysis and Multiobjective Nonlinear Model Predictive Control. Austin Chem Eng 10: 1107.

45. Upreti, Simant Ranjan (2013) Optimal control for chemical engineers. Taylor and Francis.

46. Dubey SR, Singh SK, Chaudhuri BB (2022) Activation functions in deep learning: A comprehensive survey and benchmark. Neurocomputing 503: 92-108.

47. Kamalov AF, Nazir M, Safaraliev AK, Cherukuri, R Zgheib (2021) Comparative analysis of activation functions in neural networks, 2021 28th IEEE International Conference on Electronics, Circuits, and Systems (ICECS), Dubai, United Arab Emirates 1-6.

48. Szandała T (2020) Review and Comparison of Commonly Used Activation Functions for Deep Neural Networks. ArXiv.

49. Sridhar LN (2023) Bifurcation Analysis and Optimal Control of the Tu¬mor Macrophage Interactions. Biomed J Sci & Tech Res BJSTR 53.

50. Sridhar LN (2024) Elimination of oscillation causing Hopf bifurcations in engineering problems. Journal of Applied Math 2: 1826.